BEN-GURION UNIVERSITY OF THE NEGEV
FACULTY OF ENGINEERING SCIENCES
DEPARTMENT OF BIOMEDICAL ENGINEERING

Diffusion in Inhomogeneous Systems

Thesis submitted in partial fulfillment of the requirements for the M.Sc degree

By: Shaked Regev

May, 2017

BEN-GURION UNIVERSITY OF THE NEGEV

FACULTY OF ENGINEERING SCIENCES

DEPARTMENT OF BIOMEDICAL ENGINEERING

Diffusion in Inhomogeneous Systems

Thesis submitted in partial fulfillment of the requirements for the M.Sc. degree

By: Shaked Regev

Supervised by: Prof. Oded Farago

Author:..... Date:.....

Supervisor:..... Date:.....

Chairperson of the committee

for graduate studies:..... Date:.....

May, 2017

Abstract

Single-particle diffusion, also known as Brownian motion, is the random motion of a particle in space due to collisions with its surrounding medium. The theory of diffusion in a homogeneous medium, one with a constant diffusion coefficient, is well established and recognized. The theoretical basis of diffusion in heterogeneous environments, where the diffusion coefficient varies in space, is far less developed. In this thesis, we employ underdamped Langevin dynamics simulations and analytical methods for studying these systems, which are common in many fields, including biomedical engineering. We investigate two model systems: The first is the dynamics of Brownian particles in a heterogeneous one-dimensional medium with a spatially-dependent diffusion coefficient of a power-law form, at constant temperature. At long times, provided that the friction coefficient drops slowly enough (or grows at any rate), both approaches yield identical results, corresponding to subdiffusion or superdiffusion. In the opposite case, where the friction coefficient decays more quickly, the diffusion equation foresees that the particles accelerate, while the Langevin equation predicts ballistic motion at long times. We argue that the phenomenon of particle acceleration in an isothermal medium is unphysical, and demonstrate that in this case underdamped Langevin dynamics simulations must be used. In the second case study, we use a one-dimensional two layer model with a semi-permeable membrane to model the diffusion of a therapeutic drug delivered from a drug-eluting stent (DES). The rate of drug transfer from the stent coating to the arterial wall is calculated by using underdamped Langevin dynamics simulations. Our results reveal that the membrane has virtually no delay effect on the rate of delivery from the DES.

Acknowledgments

I would like to express my sincerest gratitude to my supervisor, Prof. Oded Farago, for all the guidance, advice, support, encouragement, assistance, and constructive criticism he has offered me throughout the two years of my thesis.

I am particularly thankful for the assistance and advice of my lab associate, Nadiv Dharan, as well as the fruitful discussions we have had over the past two years.

Contents

1 Introduction **7**

1.1 Brownian dynamics in uniform systems 7

1.2 Spatially-dependent friction 11

1.3 Numerical integration 13

1.4 Thesis Outline 15

2 Isothermal Langevin dynamics in systems with power-law spatially dependent friction 16

2.1 Introduction 16

2.2 Heterogeneous media with power law friction function 19

2.2.1 Fick's second law 19

2.2.2 Langevin Dynamics Simulations 20

2.3 Ballistic Motion 22

2.3.1 The case $c \geq 1$ 22

2.3.2 Crossover to ballistic motion 24

2.3.3 The fluctuation-dissipation relationship 27

2.4 Summary and Discussion 28

3 Application of underdamped Langevin dynamics simulations for the study of diffusion from a drug-eluting stent **31**

3.1 Introduction 31

3.2 Two-layer systems 32

3.3 Semi-permeable membrane 35

3.4 Two-layer stent model 37

3.4.1 The model 37

3.4.2 Using a fictitious mass 38

3.4.3 Membrane permeability 40
3.5 Results 41
3.6 Discussion 43

4 Summary **46**

A Diffusion in higher dimensions **48**

Chapter 1

Introduction

1.1 Brownian dynamics in uniform systems

Diffusion (from the Latin *diffundere*- to spread or pour out) describes the random motion of particles in space, also known as Brownian motion. Brownian motion was first observed by the botanist Brown while examining the motion of pollen grains under a microscope, and noticing their random jitter in water [1]. Years later, an explanation for this observation was given by Einstein, who traced it to the random collisions between the grains and the water molecules [2]. These collisions cause the Brownian particle to exhibit random motion, also known as single-particle diffusion. When many particles display this type of motion, they generate a net flow of particles from an area with a high concentration, or a large chemical potential, to an area with a low concentration or a small chemical potential. This phenomenon is also referred to as moving down the concentration or chemical potential gradient.

Particle transport via diffusion is relevant in a variety of different fields such as physics, chemistry [3], electrical engineering [4], material science [5], and mechanical engineering [6]. It is appropriate not only for translational motion, but also for rotational motion [7] and even for momentum variation [8]. The term 'diffusion' is used more broadly in a non-

physical sense, e.g., in the context of sociology, economics, and ecosystems, to describe the spreading of populations and ideas [9]. Diffusion is relevant in the biomedical field since it is a predominant transport process in cell biology and physiology [10]. It is also central in many biomedical applications, e.g., in drug eluting stents [11], transdermal biotechnologies [12], and diffusion near a wall [13].

Returning to Brownian motion of particles, the process of diffusion may be described in one of two ways, via Langevin's equation [14] or a continuum approach, tied to Fick's laws of diffusion [15]. Fick's first law of diffusion describes the relationship between the flux of particles J and the spatial derivative of the probability distribution function (PDF) of the particles $P(x,t)$: $J(x,t) = -D\vec{\nabla}P(x,t)$, where x and t respectively denote coordinate and time, and D is the diffusion coefficient. Fick's second law relates the spatial derivative of the flux and the time derivative of the PDF and reads

$$\frac{\partial P(x,t)}{\partial t} = -\vec{\nabla}J = D\nabla^2 P(x,t). \tag{1.1}$$

In one dimension (1D), assuming a Dirac delta-function initial condition $P(x,0) = \delta(x)$, the solution of Eq. (1.1) is given by the normal distribution $P(x,t) = (4\pi Dt)^{-0.5}\exp\left(-x^2/4Dt\right)$. The mean displacement of the Brownian particle $\langle \Delta x \rangle = 0$, while the mean squared displacement (MSD) grows linearly with time:

$$\left\langle \Delta x^2 \right\rangle = 2Dt, \tag{1.2}$$

The linear growth of the MSD is a defining characteristic of normal diffusion. In 3D $\langle \Delta x^2 \rangle = \langle \Delta y^2 \rangle = \langle \Delta z^2 \rangle = 2Dt$ and, therefore, $\langle \Delta r^2 \rangle = 6Dt$.

The particle approach for describing Brownian motion is based on the Langevin equation of motion [14]

$$m\frac{dv}{dt} = -\alpha v + \beta(t), \tag{1.3}$$

where m and v denote, respectively, the mass and velocity of the particle. This description is essentially Newton's second law applied to each particle. It would, more generally, include an independent force $f(x,t)$, which throughout this thesis is zero, since we consider only free diffusion. The impact of the random collisions on the Brownian particle is realized through the action of two forces, represented by the terms on the r.h.s. (right hand side) of the equation. The first is a friction force representing the statistical average of the collision forces, while the second is a random Gaussian white noise accounting for the force distribution around the mean value. The Gaussian white noise term in Langevin's equation has the following statistical properties [16]: $\langle\beta(t)\rangle = 0$, and $\langle\beta(t)\beta(t')\rangle = 2B\delta(t-t')$, where $\langle\cdots\rangle$ denotes the average over all possible realizations of the noise force $\beta(t)$.

Since the magnitude of the collision forces depends on the characteristic thermal velocity of the molecules of the embedding fluid, the friction coefficient α in Langevin's equation (1.3) must depend on the temperature, T. It should also be related to the diffusion coefficient, D, appearing in Eq. (1.1). The relation, $\alpha = k_B T/D$ (where k_B is Boltzmann's constant), is known as Einstein's relation, which is closely related to the more general fluctuation-dissipation theorem [17]. Using the formal solution for Eq. (1.3)

$$v(t) = e^{-\alpha t/m}v(0) + \int_0^t dt' e^{-\alpha(t-t')/m}\frac{\beta(t')}{m} \tag{1.4}$$

we can prove that $B = \alpha k_B T$ as follows: Squaring and taking the average of Eq. (1.4) yields $\langle v^2\rangle = k_B T/m$ (according to the equipartition theorem) on the left hand side. On the right hand side we have the following three terms:

$$\left\langle e^{-2\alpha t/m}v^2(0)\right\rangle \to 0, \tag{1.5}$$

for $t \to \infty$,

$$2e^{-\alpha t/m}v(0)\int_0^t dt' e^{-\alpha(t-t')/m}\langle\beta(t')\rangle/m = 0, \tag{1.6}$$

since $\langle\beta(t)\rangle = 0$, and

$$\tfrac{1}{m^2}\left\langle \int_0^t dt' e^{-\alpha(t-t')/m}\beta(t') \int_0^t dt'' e^{-\alpha(t-t'')/m}\beta(t'')\right\rangle . \tag{1.7}$$

Recalling that $\langle\beta(t)\beta(t')\rangle = 2B\delta(t-t')$, Eq.(1.7) becomes

$$\frac{2B}{m^2}\int_0^t dt' e^{-2\alpha(t-t')/m} = \frac{B}{\alpha m}(1-e^{-2\alpha t/m}), \tag{1.8}$$

which for $t \to \infty$ converges to $B/(\alpha m)$. Recall that this must equal k_BT/m. Therefore, $B = \alpha k_B T$ and $\langle\beta(t)\beta(t')\rangle = 2\alpha k_B T\delta(t-t')$. Notice that for this value of B, $\langle v^2\rangle = k_BT/m$ for all t, since Eq.(1.5) and the second term in Eq.(1.8) cancel out exactly.

The particle's MSD can be obtained in a similar fashion, by substituting Eq. (1.4) in $x(t) = x_0 + \int_0^t v(t')dt'$ and simplifying:

$$x(t) = x_0 + \frac{v_0 m}{\alpha}\left[1-e^{-\alpha t/m}\right] + \frac{1}{\alpha}\int_0^t dt' e^{-\alpha(t-t')/m}\beta(t'). \tag{1.9}$$

We are interested in $\langle\Delta x^2\rangle$, the MSD of the particle, where $\Delta x = x - x_0$. Subtracting x_0, squaring and taking the average of Eq. (1.9) yields:

$$\left\langle\Delta x^2\right\rangle = \frac{m^2}{\alpha^2}\left[1-e^{-\alpha t/m}\right]\left[\left\langle v_0^2\right\rangle - \frac{k_BT}{m}\right] + \frac{2k_BT}{\alpha}\left[t - \frac{m}{\alpha}\left(1-e^{-\alpha t/m}\right)\right]. \tag{1.10}$$

At equilibrium ($\langle v_0^2\rangle = k_BT/m$), the first term vanishes, which leaves:

$$\left\langle\Delta x^2\right\rangle = \begin{cases} \frac{k_BT}{m}t^2 & t \to 0 \\ 2\frac{k_BT}{\alpha}t & t \to \infty\ . \end{cases} \tag{1.11}$$

Comparing Eq. (1.11) to Eq. (1.2), we can infer the Einstein relation $\alpha = k_BT/D$.

From Eq. (1.11) we read that the dynamics is diffusive only on large time scales. On short time scales, Langevin dynamics is ballistic (inertial). These properties are evident in the MSD, Eq.(1.11). The crossover between the ballistic and diffusive regimes occurs at

$\tau \sim m/\alpha$, the characteristic time of the exponent in Eq. (1.10), also known as the ballistic time. The correspondence between the diffusion equation (1.1) and Langevin's equation (1.3) holds only in the diffusive regime. However, typically, there is a clear separation of many orders of magnitude between the microscopic ballistic time and the macroscopic time of interest. [18]. Additionally, the equation neglects the influence of the motion of the Brownian particle on the embedding fluid. The fluid acts as an ideal heat bath whose properties remain unaffected by the presence of the moving Brownian particle. This latter assumption is justified when the number of fluid molecules is macroscopically large, and when the momentum and energy are locally transferred to the bulk fluid much faster than any other relevant time scale of the dynamics.

1.2 Spatially-dependent friction

Model systems with spatially dependent diffusivity have been receiving renewed interest recently due to their relevance to single-particle experiments involving femto-Newton force measurements [19,20]. So, we now consider Brownian dynamics in a medium with a position-dependent friction coefficient $\alpha(x)$. These types of dynamics are often associated with the Itô-Stratonovich dilemma [21]. The dilemma itself is not the main topic of this thesis, and we refer the reader to textbooks on stochastic dynamics [3, 4], for more details. Here we only give a brief account of the issues relevant to this work. The generalization of Eq. (1.3) corresponding to dynamics of Brownian particles, at constant temperature, in (1D) systems with spatially-dependent friction coefficients, is [22, 23]

$$m\frac{dv}{dt} = -\alpha(x)v + \beta\left(x\left(t\right)\right), \tag{1.12}$$

with $\alpha(x) = k_B T/D(x)$, which is a natural generalization of Einstein's relation [24]. As one is typically interested only in the large temporal diffusive regime, a common practice is to

look at the overdamped (non-inertial) limit of Eq. (1.12) corresponding to $m(dv/dt) = 0$,

$$0 = -\alpha(x)v + \beta\left(x\left(t\right)\right). \tag{1.13}$$

When the Eq. (1.12) is integrated over time in order to calculate the trajectory of the particle [25], one has to supplement the equation with a convention (rule) for choosing the value of α during each integration time step dt. This requirement arises since the value of $\alpha(x)$ changes during this time step. The name "Itô-Stratonovich dilemma" assigned to the ambiguity about the choice of interpretation is after the two most commonly used conventions - the one of Itô [26] which uses the value of α at the beginning of the time step, and the one of Stratonovich [27] which takes the average of the friction function at the initial and the end points. In the overdamped limit, i.e. Eq. (1.13), different conventions lead to trajectories with different statistical properties, even for $dt \to 0$ [28]. Numerical integration of Eq. (1.13) using the Itô convention yields the PDF which solves the equation:

$$\frac{\partial P(x,t)}{\partial t} = \frac{\partial^2\left(D(x)P(x,t)\right)}{\partial x^2}, \tag{1.14}$$

while numerical integration using the Stratonovich convention yields the PDF which solves the equation:

$$\frac{\partial P(x,t)}{\partial t} = \frac{\partial}{\partial x}\left(\sqrt{D\left(x\right)}\frac{\partial\left(\sqrt{D\left(x\right)}P(x,t)\right)}{\partial x}\right). \tag{1.15}$$

The equation correctly describing Brownian dynamics at constant temperature is Fick's equation:

$$\frac{\partial P(x,t)}{\partial t} = \frac{\partial}{\partial x}\left(D\left(x\right)\frac{\partial P(x,t)}{\partial x}\right). \tag{1.16}$$

The convention that produces the same PDF is neither Itô's nor that of Stratonovich, but rather Hänggi's interpretation (also known as the "isothermal" convention) [29, 30] which uses α at the end of the time step [22, 23]. In the case of underdamped Langevin dynamics [i.e., Eq. (1.12) with the l.h.s. *not* assumed to be vanishingly small], all (reasonable) conventions [31] converge to the correct PDF in the limit $dt \to 0$. This difference between underdamped dynamics and its overdamped limiting case stems from fact that in the latter, the velocity is physically ill-defined (since it is proportional to the white noise β), while in the former, it remains finite and follows the equilibrium Maxwell-Boltzmann distribution. Formally (mathematically) speaking, there is no dilemma in the second-order (in x) equation (1.12). However, the rate of convergence of numerical simulation-results toward the theoretical PDF [i.e., the solution of Eq. (1.16)] greatly depends on the chosen convention and the numerical integrator. This issue has considerable practical importance in numerical simulations where the time step dt is not infinitesimal. The results in the work are based on Langevin dynamics simulations employing the G-JF integrator [32,33] with a newly proposed "inertial" convention [22,24] (to be discussed in the following section 1.3). This combination produces excellent results even for relatively large integration time steps.

1.3 Numerical integration

The PDF in Langevin dynamics simulations can be obtained from an ensemble of trajectories of particles starting at x^0 drawn from the initial distribution $P(x, 0)$, with initial velocities, v^0, taken from an equilibrium Maxwell-Boltzmann distribution. The trajectories are computed by numerically integrating Langevin's equation of motion (1.12). Denoting, respectively, by x^n and v^n the position and velocity of a particle at time t_n, the integration is conducted using the G-JF algorithm that advances the system by one time step to

$t_{n+1} = t_n + dt$, using the following set of discrete-time equations [32, 33]:

$$x^{n+1} = x^n + bdtv^n + \frac{bdt^2}{2m} f^n + \frac{bdt}{2m}\beta^{n+1} \tag{1.17}$$

$$v^{n+1} = av^n + \frac{dt}{2m}\left(af^n + f^{n+1}\right) + \frac{b}{m}\beta^{n+1}, \tag{1.18}$$

where $f^n = f(x^n)$ is the *deterministic* force acting on the particle, β^{n+1} is a Gaussian random number with

$$\langle \beta^n \rangle = 0 \; ; \; \left\langle \beta^n \beta^l \right\rangle = 2\alpha k_B T dt \delta_{n,l}, \tag{1.19}$$

and the damping coefficients of the algorithm are

$$b = \left[1 + (\alpha dt/2m)\right]^{-1} \; ; \; a = \left[1 - (\alpha dt/2m)\right] b. \tag{1.20}$$

We set $f^n = 0$ since we consider the case when the particle experiences no forces other than random collisions with the fluid molecules.

Since the friction coefficient varies in space, the above equations (1.17) and (1.18) must be complemented with a convention for choosing the value of α to be used in Eqs. (1.19) and (1.20) at each time step. Here, we use the recently proposed inertial convention that assigns to α the value of the spatial average of the friction function along the inertial trajectory from x^n to $\tilde{x}^{n+1} = x^n + v^n dt$ [22, 24]

$$\frac{\int_{x^n}^{\tilde{x}^{n+1}} \alpha(x) dx}{\tilde{x}^{n+1} - x^n} = \frac{A(\tilde{x}^{n+1}) - A(x^n)}{\tilde{x}^{n+1} - x^n}, \tag{1.21}$$

where $A(x)$ is the primitive function of $\alpha(x)$. We have previously demonstrated that the combination of the G-JF algorithm with the inertial convention produces excellent agreement between the computed and theoretical PDFs, even for relatively large intergration time steps.

1.4 Thesis Outline

In this work, we present two case studies of diffusion in one-dimensional model systems. The first example [34], discussed in chapter 2, is concerned with the dynamics of a particle in a medium with a spatially-dependent diffusion coefficient, $D(x) \propto |x|^c$. In this example, the particle does not exhibit the features of normal diffusion, but, depending on the exponent c, is rather characterized by sub- or super-diffusive motion. In the second example, discussed in chapter 3, we consider the biomedical problem of drug transport from a drug-eluting stent. This is done by considering a simple two-layer model system, representing the drug coating and arterial wall, with a semi-permeable membrane, representing the drug topcoat, between them. Finally, in chapter 4, we summarize the main conclusions of this work and discuss potential future research directions.

Chapter 2

Isothermal Langevin dynamics in systems with power-law spatially dependent friction

2.1 Introduction

Anomalous diffusion processes differ from normal diffusion processes in that their MSD grows non-linearly with time, i.e.:

$$\left\langle \Delta x^2 \right\rangle \propto t^k, \tag{2.1}$$

with $k < 1$ corresponding to sub-diffusion and with $k > 1$ for super-diffusion. Anomalous diffusion emerges in different fields, for instance daily fluctuations in climate variables such as temperature [35] or the plume growth in the atmosphere [36], stock price variations [37], diffusion in disordered media [38] and worm-like micellar solutions [39], and the movement of ultra-cold atoms [40]. Another example of sub-diffusion is the scaling behavior of the center of mass of a flexible polymer at short times. In the bead and spring or Rouse model $k = 1/2$ in Eq. (2.1), while the Zimm model, which takes hydrodynamic interactions into account,

yields $k = 2/3$ [41, 42]. In biological systems, the phenomenon of sub-diffusion has lately been observed in systems such as single particle diffusion in cytoplasm [43], and telomeres in cell nuclei [44]. Super-diffusion in biology was also noticed in active cellular transport processes [45], for instance, in the motion of micron-scaled beads in a bacterial bath at short times [46], and in the food foraging locomotion of animals such as *Drosphilia* fruit flies [47].

Although any dynamics with MSD $\langle \Delta x^2 \rangle \propto t^k$, for $k \neq 1$, is considered anomalous diffusion, there are several distinct approaches to stochastic dynamics. One framework for anomalous diffusion is the continuous time random walk (CTRW) formalism, which is a generalization of a random walk where a particle is delayed by a certain random time between successive steps. This formalism has been used for describing several phenomena such as transport in amorphous materials [48] and variations in currency exchange rates [49]. The diffusion equation describing CTRW is given in ref. [50]:

$$\frac{\partial}{\partial t} P(x,t) = D \rho_t^{1-2H} \frac{\partial^2}{\partial x^2} P(x,t), \tag{2.2}$$

where ρ_t^{1-2H} is the Riemann-Liouville fractional operator defined as [51, 52]

$$\rho_t^{1-2H} P(x,t) = \frac{1}{\Gamma(2H)} \frac{\partial}{\partial t} \int_0^t \frac{P(x,t')}{(t-t')^{1-2H}} dt', \tag{2.3}$$

and $0 < H < 1$ is called the Hurst parameter. The MSD in this case is highly dependent on the distribution of wait times. A distribution with a finite second moment ($H \geq 0.5$) will lead to normal diffusion; however, choosing wait times distributed by $\Psi(t) \propto t^{-1-2H}$ with $0 < H < 0.5$ will lead to $\langle \Delta x^2 \rangle \propto t^{2H}$, or sub-diffusion [53].

A Lévy walk, where a particle can make l correlated steps in the same direction with probability $p \propto l^{-2-\beta}$ and otherwise makes a random step in any direction, is an additional framework which gives rise to anomalous diffusion. In order to simulate such a walk, one should follow the following steps: (1) Take a step in either direction with the same probability and set $l = 1$. (2) Take a step in the same direction as the last step with probability $p \propto l^{-2-\beta}$

and take a step in either direction (with the same probability) with probability $1-p$. (3) If the current step was in the same direction as last step set $l = l+1$; otherwise, set $l = 1$. Go to step 2. In Lévy walks, the MSD scales as a power-law of the time [54]:

$$\left\langle \Delta x^2 \right\rangle = \begin{cases} t^2 & -1 < \beta \leq 0 \\ t^{2-\beta} & 0 < \beta < 1 \\ t \ln t & \beta = 1 \\ t & \beta > 1 \end{cases} \tag{2.4}$$

Eq. (2.4) shows that, in contrast to CTRWs, during a Lévy walk, a particle can experience ballistic motion for $-1 < \beta \leq 0$, super-diffusion for $0 < \beta \leq 1$, and normal diffusion for $\beta > 1$.

Another popular framework is fractional Brownian motion (fBm), which has been used to describe, e.g., anomalous diffusion in synthetic hydrology [55]. It differs from normal Brownian motion by a correlation function between two positions, $x(t_1)$, $x(t_2)$:

$$\langle x(t_1)x(t_2)\rangle = D(|t_1|^{2H} + |t_2|^{2H} - |t_1 - t_2|^{2H}). \tag{2.5}$$

For $H = 0.5$ the steps are uncorrelated (corresponding to regular Brownian motion), while for $H > 0.5$ ($H < 0.5$) they are positively (negatively) correlated. In this case $\langle \Delta x^2 \rangle \propto t^{2H}$, meaning the particle experiences sub-diffusion for $H < 0.5$ and super-diffusion for $H > 0.5$ [56–59]. FBm be described by the fractional Langevin equation [50]

$$m\frac{d^2x(t)}{dt} = -\alpha \int_0^t (t-t')^{2H-2} \left(\frac{dx(t')}{dt'}\right) dt' + \eta\xi(t), \tag{2.6}$$

where $\xi(t)$ is a power-law correlated noise kernel of the form $\langle \xi(t_1)\xi(t_2)\rangle = 2HD|t_1 - t_2|^{2H-2} + 4HD|t_1 - t_2|^{2H-1}\delta(t_1 - t_2)$, and the noise amplitude $\eta = \sqrt{\frac{\alpha^2}{2H(2H-1)}}$. The PDF which arises

from fBm is of a Gaussian form

$$P(x,t) = \frac{1}{4\pi D t^{2H}} exp\left(-\frac{x^2}{4Dt^{2H}}\right), \tag{2.7}$$

with a standard deviation that grows $\propto t^{2H}$.

Recently, it has been noticed that anomalous diffusion may also arise in heterogeneous systems with coordinate-dependent diffusivity of the power-law form: $D(x) \propto |x|^c$ [60–63]. An example where power-law diffusivity emerges (as can be realized via scaling arguments) is Brownian dynamics on fractal objects. [64]. In this chapter, we take a closer look at these types of systems, from the perspective of underdamped Langevin dynamics. In particular, we examine the prediction that for $c > 1$, the dynamics is hyper-diffusive, namely, that it is characterized by a MSD that grows faster than quadratically in time. As we will see, this result violates basic physical principles, which can be traced to the non-physical nature of the overdamped Langevin equation (1.13), that neglects the ballistic regime of the dynamics.

2.2 Heterogeneous media with power law friction function

2.2.1 Fick's second law

For $D(x) = D_0 |x/l|^c$, the solution of Eq. (1.16) is [64]

$$P(x,t) = \frac{\left[(2-c)^c D_0 t\right]^{1/(c-2)}}{2\Gamma\left(\frac{1}{2-c}\right)} \exp\left[\frac{-|x|^{2-c}}{(2-c)^2(D_0 t)}\right], \tag{2.8}$$

where Γ is the Gamma function, and for brevity we set $l = 1$. This solution satisfies the condition that the particle's motion starts at the origin: $P(x,0) = \delta(x)$. From the requirement that $P(x,t)$ vanishes for $x \to \pm\infty$, which is necessary (but not sufficient) to ensure that $\int_{-\infty}^{\infty} P(x,t)dx = 1$, we infer that the solution can be physical only for $c < 2$.

From symmetry considerations, the ensemble average $\langle x \rangle = 0$, while the MSD,

$$\left\langle \Delta x^2 \right\rangle = \int_{-\infty}^{\infty} x^2 P(x,t) dx = \frac{\Gamma\left(\frac{3}{2-c}\right)}{\Gamma\left(\frac{1}{2-c}\right)} \left[(2-c)^2 D_0 t\right]^{2/(2-c)}. \tag{2.9}$$

Thus, for $c < 0$ we observe subdiffusion, and for $0 < c < 1$ we find superdiffusion. For $c = 0$ we have $\langle \Delta x^2 \rangle = 2D_0 t$, i.e., normal diffusion, and for $c = 1$ the particle's motion is ballistic. For $c > 1$, Eq. (2.9) predicts dynamics which are faster than ballistic (for instance, $c = 1.5$ corresponds to dynamics at costant acceleration). This is an unphysical result, and in what follows we demonstrate that for any $c \geq 1$ the motion remains ballistic.

2.2.2 Langevin Dynamics Simulations

The PDF can be obtained from an ensemble of trajectories of particles starting at the origin, $x^0 = 0$, with initial velocities, v^0, drawn from an equilibrium Maxwell-Boltzmann distribution. The trajectories are computed by numerically integrating Langevin's equation of motion (1.12) by using the G-JF algorithm detailed in 1.3.

Fig. 2.1 depicts our results for the PDF for systems with a power law friction function $\alpha(x) = k_B T/D(x) = (k_B T/D_0)|x/l|^{-c}$, for $c = -0.5$ (A) and $c = +0.5$ (B). For convenience, we set $m = 1$, $D_0 = 1$, $k_B T = 1$, and $l = 1$. The results have been obtained from simulations of 2.5×10^5 trajectories with integration time step $dt = 10^{-3}$. The open circles in Figs. 1(A) and (B) represent our numerical results for the PDF at $t = 1000$ for $c = -0.5$ and $c = 0.5$, respectively. The numerical results exhibit excellent agreements with the corresponding analytical predictions of Eq. (2.8), which are plotted with the solid curves.

The symbols in Fig. 2.2 represent the numerical results for the MSD for $c = -0.5, 0.25, 0.5, 0.75$. We observe that the power-law behavior $\langle \Delta x^2 \rangle \sim t^{\frac{2}{2-c}}$ [see Eq. (2.9)], which is depicted by the lines in the figure, is indeed recovered at large times. The same power-law (2.9) was previously derived in ref. [62], where instead of Fick's law (1.16), a different diffusion equation $\partial_t P = \partial_x \left[\sqrt{D(x)}\, \partial_x \left(\sqrt{D(x)} P\right)\right]$ [Eq. (1.15)] was considered. The latter form of the dif-

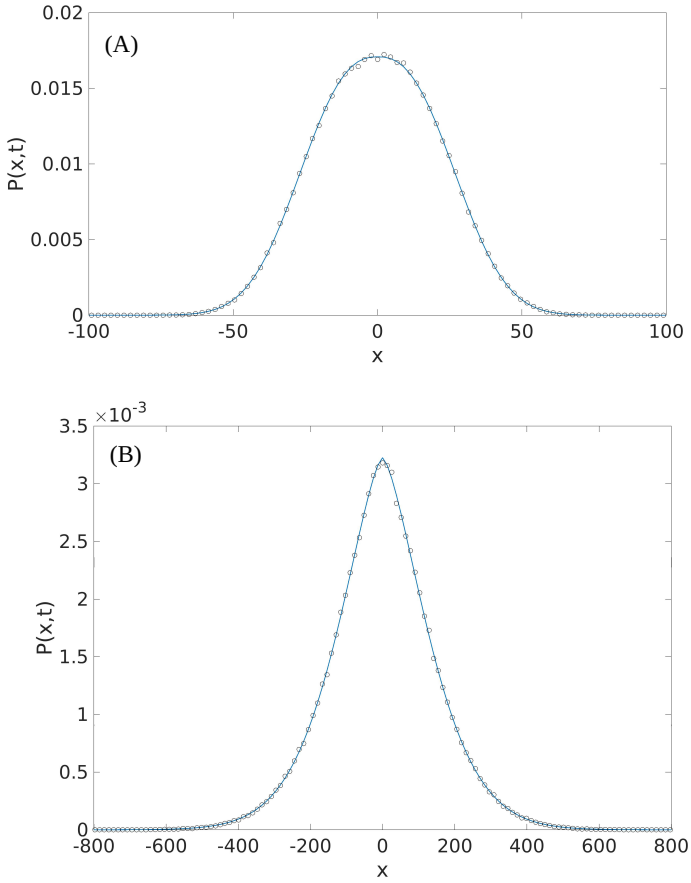

Figure 2.1: **(A)** The PDF at $t = 1000$ obtained from the numerical integration (open circles) vs. the PDF given by Eq. (2.8) (solid line), which solves Fick's diffusion equation for $c = -0.5$. **(B)** Same as **(A)**, for $c = 0.5$.

fusion equation corresponds to the Stratonovich interpretation of the overdamped Langevin equation. The reader is reminded (see section 1.2) that for overdamped Langevin dynamics, different conventions lead to different PDFs. Indeed, although both equations yield the same power-law for the MSD, the PDFs solving these equations look markedly different. Specifically, the PDFs of the Statonovich diffusion equation diverge at the origin for $c > 0$, and assume a a bimodal form for $c < 0$, with a vanishing value at the origin [62]. In contrast, the PDFs of Fick's law of diffusion (which corresponds to Hänggi's interpretation) attain a maximum at the origin. Our Langevin dynamics simulations, which at large times reproduce PDFs that agree with Eq. (2.8), serve as yet another demonstration for the appropriateness of Hänggi interpretation and Fick's second law for diffusion at constant temperature. This

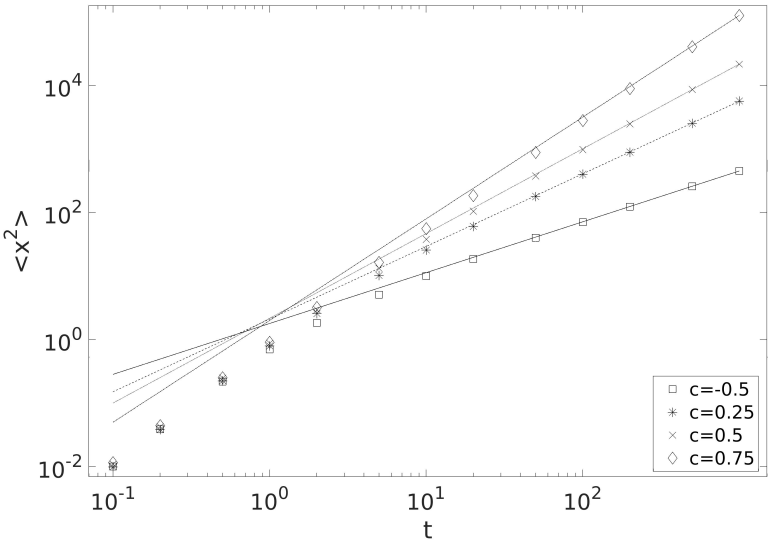

Figure 2.2: The MSD $\langle \Delta x^2 \rangle$ of the particle as a function of time for $c = -0.5, 0.25, 0.5, 0.75$ (markers), vs. the expected $\langle \Delta x^2 \rangle$ for $c = -0.5, 0.25, 0.5, 0.75$ according to Eq. (2.9) (lines).

is because the simulations follow the underdamped (inertial) Langevin dynamics of the particle. As noted above, for the inertial Langevin equation, all interpretations converge to the correct solution in the limit of small integration time steps.

2.3 Ballistic Motion

2.3.1 The case $c \geq 1$

Integrating Eq. (1.12) from the initial time to t, and taking the ensemble average over all noise realizations, yields the following relationship

$$\langle m\Delta v \rangle = -\langle \Delta A\,(x) \rangle \tag{2.10}$$

between the momentum change (force impulse) and displacement of the particle. Eq. (2.10), which was previously derived in ref. [24], involves $A(x)$ - the primitive function of $\alpha(x)$ [see

Eq. (1.21)]. This implies that $\alpha(x)$ must be an integrable function. For $\alpha(x) \sim x^{-c}$ with $c \geq 1$, the friction function is non-integrable at $x = 0$. This feature makes it impossible to start the simulations when the particle is at the origin due to the inability to define the friction coefficient for the initial step. If the particle is placed on one side of the system, it will never cross to the other side. This is because no matter how close the particle approaches to the origin, its ballistic distance (the characteristic distance that it travels before changing its direction) will always be shorter than the distance to the origin. In other words, for $c \geq 1$, the dissipation near the origin diverges so rapidly, that the singularity acts like a wall that stops the particle and bounces it back. This scenario, however, is unphysical, and it stems from the unphysical nature of Langevin's equation which only considers the influence of the medium on the particle but ignores the impact of the particle on the medium. From momentum conservation we know that any change in the momentum of the Brownian particle must be countered by an opposite change in the momentum of the molecules of the medium. This implies that when the particle is reflected from the origin, it exerts a force on the friction singularity, and this force will cause changes in the medium that would not allow the singularity to be long-lived.

Apart from the divergence of $A(x)$ at the origin, it is also interesting to consider the ramifications of the rapid drop in $\alpha(x)$ in the limits $x \to \pm\infty$. For $c > 1$, the integral over $\alpha(x)$ from $x_0 > 0$ ($x_0 < 0$) to $+\infty$ ($-\infty$) is finite, implying that the particle's ballistic distance may diverge. This can be inferred from Eq. (2.10), which suggests that it is unlikely for a particle to change its direction of motion, if it reaches x_0 with velocity $v_0 > [A(\infty) - A(x_0)]/m$. In other words - as the particle travels further away from the origin, it experiences a vanishingly small friction force and, therefore, its motion would ultimately become ballistic. The crossover from diffusive to ballistic dynamics is further explored in the following subsection.

2.3.2 Crossover to ballistic motion

We now consider dynamics in a one-dimensional system with the spatially-dependent diffusion coefficient

$$D(x) = D_0 \left[1 + \left(\frac{x}{l}\right)^2\right]. \tag{2.11}$$

For this choice, $D(x) \sim x^c$ with $c = 2$ for $x/l \gg 1$; but unlike the power-law form discussed in section 2.3.1 above, the friction coefficient, $\alpha(x) = k_B T/D(x)$, does not diverge at the origin. A special reason for choosing the specific form Eq. (2.11) is that it has been given in ref. [23] as an example of a spatially-dependent diffusion coefficient causing increasing acceleration. This result is obtained by multiplying by x^2 both sides of the diffusion equation (for $D_0 = 1$ and $l = 1$)

$$\frac{\partial P(x,t)}{\partial t} = \frac{\partial}{\partial x}\left[\left(1 + x^2\right)\frac{\partial P(x,t)}{\partial x}\right], \tag{2.12}$$

and integrating with respect to x, which yields the equation

$$\frac{\partial \left\langle \Delta x^2 \right\rangle}{\partial t} = 2 + 6\left\langle \Delta x^2 \right\rangle, \tag{2.13}$$

which has the solution

$$\left\langle \Delta x^2 \right\rangle = \left[\exp\left(6t\right) - 1\right]/3. \tag{2.14}$$

However, the prediction of Eq. (2.14) that the MSD grows exponentially with t is unphysical since it implies the emergence of two opposite currents of particles with ever-increasing velocities. One should wonder about the energy source of the exponential growth in the kinetic energy of the Brownian particles. The particles are immersed in a medium of uniform temperature serving as a heat bath, and experience no force other than random collisions with the molecules of the medium. It is impossible that through random collisions, the Brownian

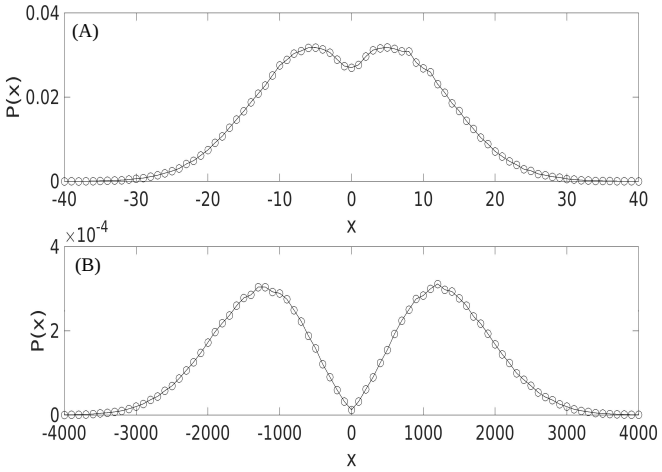

Figure 2.3: The PDF at $t = 10$ **(A)** and $t = 1000$ **(B)** of a Brownian particle starting at the origin and moving in a medium where $\alpha(x) = 1/(1 + x^2)$.

particles would consistently gain energy allowing them to reach exponentially large speeds, especially at large distances where the friction coefficient vanishes, which means that the rate of collisions with the heat bath becomes increasingly small.

The erroneous Eq. (2.14) is derived from the diffusion equation (2.12). The latter, however, does not correctly depict the dynamics of the particles in the system because it applies only to time-scales much larger than the ballistic time of the motion. As noted at the end of section 2.3.1, the ballistic distance diverges when the friction function drops faster than x^{-1} at large distances. When this occurs, the velocity of the particle saturates to some finite value, and the dynamics becomes ballistic. In other words, the ballistic time diverges, and the dynamics never reaches the diffusive regime of Eq. (2.12).

In contrast to the diffusion equation (1.16), the Langevin equation (1.12) applies to both the ballistic and diffusive regimes. Fig 2.3 presents our results for the PDF of the particles at $t = 10$ (A) and $t = 1000$ (B). The results, which are based on numerical integration of 3.25×10^5 trajectories starting at the origin (with velocities drawn from the standard Gaussian equilibrium distribution), demonstrate that as the time increases, the PDF becomes increasingly bimodal. This indicates the emergence of two opposite particle currents propagating away from the origin. Fig. 2.4(A) shows the velocity probability distribution function

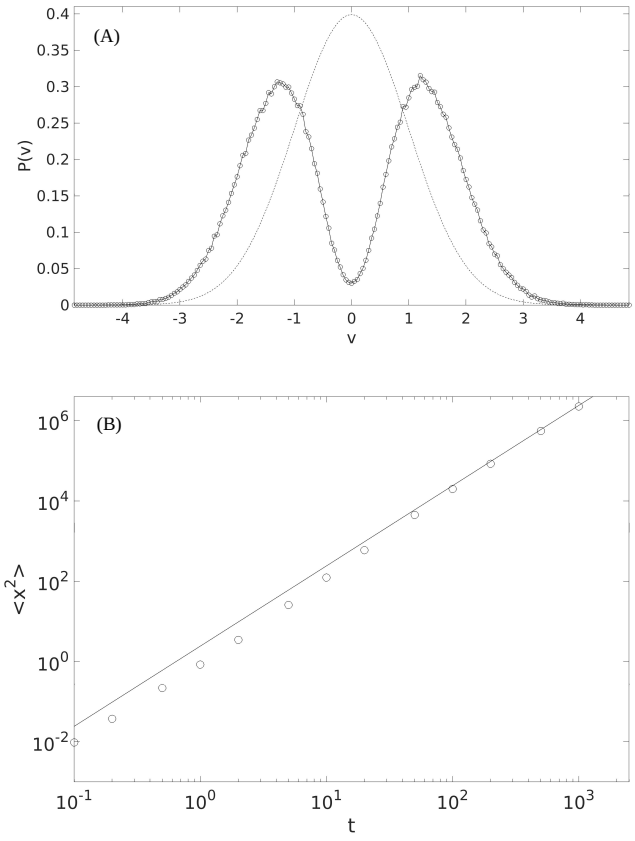

Figure 2.4: **(A)** Circles - The bimodal VPDF at $t = 1000$. The dashed line depicts the initial Gaussian equilibrium VPDF. **(B)** The computed MSD of the particle (circles) vs. the asymptotic power-law form $\langle x^2 \rangle = 2.41t^2$ (solid line).

(VPDF) at $t = 1000$ (solid circles), which is also bimodal and, thus, does not coincide with the initial equilibrium distribution (depicted by the dashed line in the figure). The VPDF at $t = 2000$ (not shown) is essentially identical to the VPDF in Fig. 2.4(A), which proves this VPDF represents the steady state of the velocity distribution. From the steady state VPDF, we find that the steady state squared velocity $\langle v^2 \rangle \simeq 2.41$ (in units of $k_B T/m$) and, therefore, at large times the position MSD $\langle x^2 \rangle = \langle v^2 \rangle t^2 = 2.41t^2$. This result, which is fully corroborated by the numerical data in Fig. 2.4(B), demonstrates that the particles end up moving inertially with velocities drawn from the steady state VPDF.

2.3.3 The fluctuation-dissipation relationship

Integrating Eq. (1.12) with respect to time, squaring the equation, and taking the ensemble average over noise realizations, yields the generalized form of the fluctuation-dissipation relationship for systems with spatially varying friction [24], which reads

$$\left\langle (m\Delta v)^2 + 2m\Delta v\Delta A + (\Delta A)^2 \right\rangle = \int_0^t 2 \left\langle \alpha \left(t' \right) \right\rangle k_B T dt'. \tag{2.15}$$

If at large times the dynamics enters the diffusive regime, the first two terms on the l.h.s. become negligible compared to the third one. Moreover, for a constant α, the third term on the l.h.s. is equal to $\alpha^2 \left\langle (\Delta x)^2 \right\rangle$, while the integral on the r.h.s. gives $2\alpha k_B T t$. Thus, for constant friction, expression (2.15) reduces (at large times) to the well-known form of the fluctuation-dissipation relationship $\left\langle (\Delta x)^2 \right\rangle = 2(k_B T/\alpha)t = 2Dt$.

For the dynamics discussed in section 2.3.2, the motion is not diffusive, but rather becomes ballistic at large times. However, relationship (2.15) holds for any time t, regardless of the character of the dynamics. This is nicely demonstrated in Fig. 2.5(A), where we plot the ensemble averages of the three terms on the l.h.s. of Eq. (2.15). As can be seen, all three terms grow rapidly at short times, which include the very initial ballistic segment, and the following interval of diffusive motion. At $t \gtrsim 100$, all three terms saturate, which indicates the crossover from diffusive to ballistic motion. In (B) we plot the sum of the averages of these three terms (dashed line) vs. the value of the r.h.s. of Eq. (2.15), which is the ensemble average of $\alpha \left(x \left(t' \right) \right)$ integrated from the beginning of the dynamics until time t (solid line). The lines overlap each other (the relative difference between them is smaller than 1%), which demonstrates that the equality between the two sides of Eq. (2.15) holds at all times.

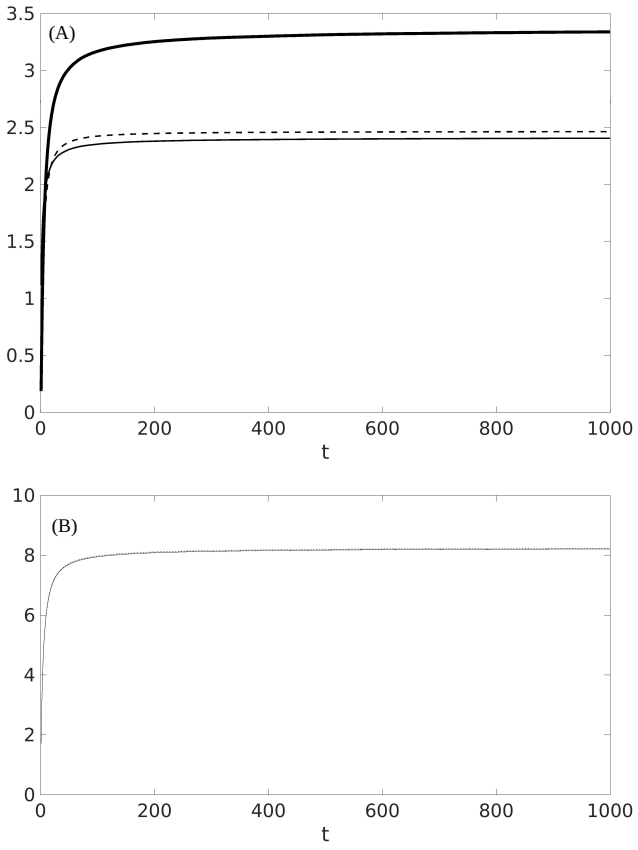

Figure 2.5: **(A)** The ensemble averages of $(m\Delta v)^2$ [first term on the l.h.s. of Eq. (2.15) - thin solid line], $2m\Delta v\Delta A$ (second term - thick solid line), and $(\Delta A)^2$ (third term - dashed line), as a function of time t. **(B)** The sum of the three averages shown in (A) (dashed line) vs. the average of $2\alpha k_B T$ integrated over time [r.h.s. of Eq. (2.15) - solid line], as a function of t.

2.4 Summary and Discussion

In this work we used computer simulations to study the Langevin dynamics of Brownian particles in a 1D system with a friction coefficient that varies as a power-law of the distance from the origin $\alpha(x) \sim |x|^{-c}$. It has been demonstrated that for $c < 1$, the particle diffuses anomalously with MSD $\langle \Delta x^2 \rangle \sim t^{2/(2-c)}$. This result can be also derived by solving the corresponding diffusion equation (1.16) with diffusion coefficient $D(x) = k_B T/\alpha(x)$.

The diffusion equation can be formally solved for $c < 2$. For $1 < c < 2$, the solution incorrectly predicts that the MSD grows faster than the MSD of ballistic motion. This result stems from the diffusion equation, which cannot be physically justified for time scales smaller

than the ballistic time of the motion. For constant friction coefficient α, a crossover from ballistic to diffusive motion occurs on time scales $\tau \geq m/\alpha$. In the case when $\alpha(x) \sim |x|^{-c}$ with $c > 1$, the friction vanishes rapidly at large distance and an opposite crossover, from diffusive back to ballistic motion, takes place. When this happens, the diffusion equation can no longer be used if the ballistic time diverges, in which case the motion remains ballistic (as the particle escapes to infinity).

In the example discussed in section 2.3.2, the divergence of the friction at the origin is removed, while at large distances $\alpha(x) \sim |x|^{-2}$. Even if the friction never vanishes completely, it drops at such a fast rate that it quickly becomes irrelevant. Thus, this example resembles dynamics of a Brownian particle in a finite fluid drop held at constant temperature T. When the particle reaches the surface of the drop, it escapes, and its velocity no longer changes. At the moment of escape the particle has to have a velocity component directed outwards from the drop and, therefore, the velocity distribution function outside of the drop differs from the equilibrium Gaussian equilibrium velocity distribution at temperature T [see Fig. 2.4(A)]. Noticeably, the mean kinetic energy of the escaping particle is larger than the corresponding equilibrium value, $dk_BT/2$ (where d is the dimentionality of the system). The fact that, on average, the escaping particle takes away an amount of kinetic energy larger than the equilibrium value implies that the molecules of the fluid drop are left with an average kinetic energy smaller than the equilibrium value. The drop cools down slightly, and in order to maintain the temperature at T, it must be connected to a true heat reservoir that would supply the missing energy. This consideration is missing in the framework of Langevin's equation that completely neglects the influences of the Brownian particle on the surrounding medium.

Finally, we note that, within the framework of Langevin dynamics, a generalized form of the fluctuation-dissipation relation has been previously derived [Eq. (2.15)]. This form holds for dynamics in media with spatially varying friction, at all times (i.e., both within the ballistic and diffusive regimes of the dynamics). If $\alpha(x)$ is bound between two positive

values, the motion at large times becomes diffusive. In such a case, the l.h.s. of Eq. (2.15) becomes dominated by the third term, and both sides of the equation grow linearly with t. Anomalous diffusion is observed when at large distances $\alpha(x) \sim |x|^{-c}$ with $c < 1$. In this case, the third term still dominates the other two terms on the l.h.s.; however, the large time behavior scales like $x^{2(1-c)} \sim t^{2(1-c)/(2-c)}$. For $c \geq 1$, the motion becomes ballistic at large times. In this case, all terms on the l.h.s. are equally important and, like the r.h.s. of the equation, relax to constant asymptotic values.

Chapter 3

Application of underdamped Langevin dynamics simulations for the study of diffusion from a drug-eluting stent

3.1 Introduction

Arterial stents are indispensable in the treatment of coronary artery disease (CAD) and more specifically stenosis, the abnormal narrowing of blood vessels [65]. These stents are frequently implanted in arteries where blood flow has become precariously impeded. In recent decades, they have revolutionized the treatment of stenosis by providing a safer alternative to coronary surgery. In addition to diminishing the risk of major surgery complications, stents also facilitate recovery and help avoid administering general anesthesia to patients [66]. However, arterial stents have only been able to reduce the instances of recurring stenosis, or restenosis, to 20-30%, compared to 30-40% in coronary surgery [67].

In an effort to further curtail these rates, drug-eluting stents (DES) were introduced. A DES is a stent that uses programmed pharmacokinetics to release anti-proliferative pharmaceuticals into the arterial wall. It is comprised of a metallic strut coated with a polymeric

matrix or gel that encapsulates the therapeutic drug [68]. The drug reduces smooth muscle cell growth and prevents an inflammatory response - two predominant causes of in-stent-restenosis and neo-intima proliferation [68]. Stents coated in anti-proliferative agents have mitigated instances of restenosis to roughly 5% in clinical trials and are FDA approved [69].

Understanding the rate at which drugs are transported through the arterial tissue is crucial for stent design, and as such has been studied extensively [11, 70–96]. The dominant mechanism of drug transfer from the coating is diffusion through the arterial wall. Thus, the simplest model describing the system is based on the solution of a diffusion equation in a two-layer one-dimensional system. More complex models give weight to other phenomena and factors such as chemical reactions between the drug and the arterial wall [70–78], directed advection of the drug [11, 70–72, 75–84], cell metabolism [79, 82], and the drug topcoat membrane permeability [11, 75, 78, 85, 86]. These phenomena and factors amend the partial differential equations (PDEs) that describe the transport of the drug. They also modify the boundary conditions between the layers and often require the introduction of additional layers [70, 71, 80, 83, 85, 87–90]. Some studies consider more complex two- [77, 89, 91] and even three-dimensional [76, 82, 85, 92, 93] geometries. The PDEs are often solved by separation of variables, or numerically through some kind of a discretization scheme, e.g., finite elements, finite differences, and the marker cell method. Noteworthy exceptions include analytical Laplace transform solutions [90], Boltzmann reductions [74], and numerically solved Voltera integral equations [86]. Experimental data is also available [94–96], and has been used to test and validate theoretical models.

3.2 Two-layer systems

Assuming in Eq. (1.16) that $0 < D(x) < \infty$ $(-\infty < x < \infty)$, the resulting $P(x,t)$ (for $t > 0$) must be a continuous function for any intial condition. The flux $j(x,t) = -D(x)\partial_x P(x,t)$ must also be continuous if no source or sink of probability are present in the system. These

properties of the PDF also apply to layered systems where D is piece-wise constant. In this section, we consider a simple one-dimensional two-layer model for a DES. Before arriving at that model, we first consider the simplest two-layer system, where $D(x) = D_1$ for $x < 0$ and $D(x) = D_2$ for $x > 0$. As just stated above, both the PDF and the flux must be continuous, including at $x = 0$, which sets the boundary conditions at the interface between the layers. Assuming that a particle is initially located at $x = x_0 > 0$, i.e., $P(x, 0) = \delta(x - x_0)$, then the *normalized* (i.e., satisfying $\int_{-\infty}^{\infty} P(x,t)dx = 1$) solution of (1.16) for $t > 0$ is given by

$$P(x,t) = \begin{cases} \frac{A}{\sqrt{4\pi D_1 t}} e^{-\frac{(x-x_1)^2}{4D_1 t}} & x < 0 \\ \frac{1}{\sqrt{4\pi D_2 t}} e^{-\frac{(x-x_0)^2}{4D_2 t}} + \frac{B}{\sqrt{4\pi D_2 t}} e^{-\frac{(x+x_0)^2}{4D_2 t}} & x > 0 \ , \end{cases} \tag{3.1}$$

with $x_1 = x_0\sqrt{D_1/D_2}$, $A = 2/(1+\sqrt{D_2/D_1})$, and $B = (1-\sqrt{D_1/D_2})/(1+\sqrt{D_1/D_2})$. This solution can be interpreted as follows: For $x > 0$, the PDF is the outcome of two diffusion processes associated with (i) the original particle which has a unity weight and is located at $x = x_0$, and an image particle of weight B located at $x = -x_0$. For $x < 0$, the PDF represents diffusion of an image particle of weight $A = 1 - B$, which is located at $x = x_1$. Notice that for $D_1 = D_2$, we have $x_1 = x_0$, $A = 1, B = 0$, which reduces Eq. (3.1) to the well-known Gaussian solution for a particle diffusing in an infinite space with constant diffusivity. Fig. 3.1 compares the PDF (3.1) for $D_1 = 1$, $D_2 = 0.1$, and $x_0 = 4$ (lines) to the results of Langevin dynamics simulations based on the above described G-JF integrator with the inertial convention (symbols). In the simulations, we set $m = 1$ and $k_BT = 1$. Thus, the friction coefficients in the layers are given by $\alpha_1 = k_BT/D_1 = 1$ and $\alpha_2 = k_BT/D_2 = 10$. We set the time step to $dt = 0.1$. For both layers, this value of dt satisfies the condition $dt \leq 2m/\alpha$, which has been assumed in the application of the inertial convention for choosing $\bar{\alpha}$ (see discussion at the end of section 1.3). Fig. 3.1 depicts the PDF at $t = 100$ and $t = 1000$, based on 2.5×10^5 trajectories. The total CPU time of the simulations was 3 minutes on a PC. The agreement with Eq. (3.1) is excellent. Interestingly, we obtained almost identical results with $dt = 4$, which does not satisfy the condition for inertial dynamics. In the latter

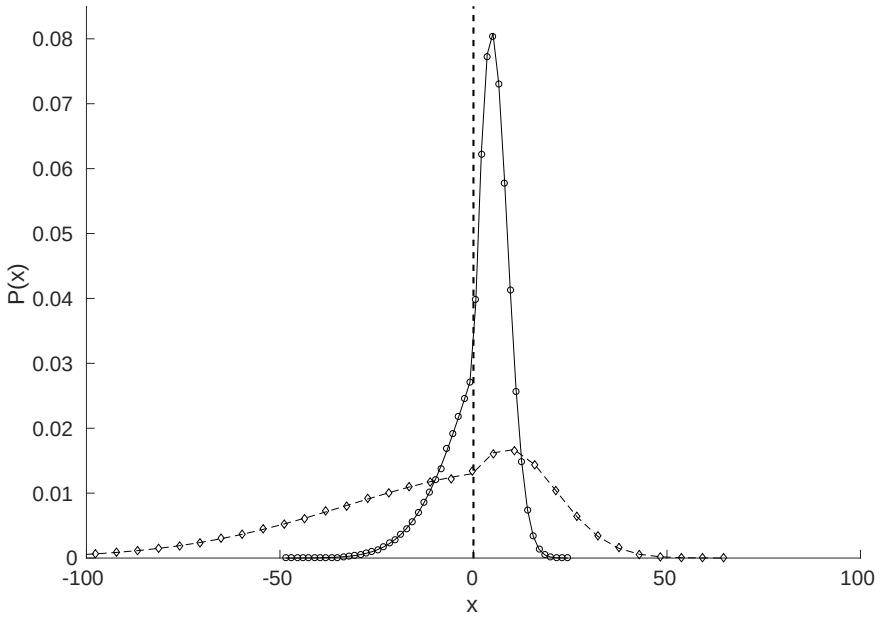

Figure 3.1: The PDF of the two-layer problem (the vertical line at $x = 0$ represents the interface). Open circles and the solid line denote, respectively, the results of the Langevin dynamics simulations and the analytical solution Eq. (3.1) at $t = 100$. Similarly, the open diamonds and the dashed line denote results for $t = 1000$.

case, the total duration of the simulations was 5 seconds.

Two interesting limiting cases may be considered: For $D_2/D_1 \to \infty$ ($D_2 = D$, $D_1 \to 0$), we have $B \to 1$, and

$$P(x,t) = \frac{1}{\sqrt{4\pi D_2 t}} e^{-\frac{(x-x_0)^2}{4D_2 t}} + \frac{1}{\sqrt{4\pi D_2 t}} e^{-\frac{(x+x_0)^2}{4D_2 t}} \quad (x > 0), \tag{3.2}$$

which is the solution of the same problem with a reflecting wall at the origin. To simulate Langevin dynamics in the presence of a reflecting wall (located, without loss of generality, at $x = 0$), we follow the trajectory of the particle as computed by the Langevin integrator. If it crosses the wall, i.e., when $x^{n+1} < 0$, we simply relocate the particle at $-x^{n+1} > 0$, and reverse the velocity from v^{n+1} to $-v^{n+1}$. The other limiting case is $D_2/D_1 \to 0$ ($D_2 = D$,

$D_1 \to \infty$). Here, we have $B \to -1$, and

$$P(x,t) = \frac{1}{\sqrt{4\pi D_2 t}} e^{-\frac{(x-x_0)^2}{4D_2 t}} - \frac{1}{\sqrt{4\pi D_2 t}} e^{-\frac{(x+x_0)^2}{4D_2 t}} \quad (x > 0), \tag{3.3}$$

which is the solution of the same problem with an absorbing wall at the origin. When one simulates Langevin dynamics with absorbing boundaries, the trajectory is terminated when it crosses the boundary. Obviously, the total probability is not conserved but rather diminishes with time.

3.3 Semi-permeable membrane

Drug-eluting stents include a topcoat that influences the rate of drug release to the artery. Since the topcoat layer is thin compared to the dimensions of the stent and the arterial wall, it can be included in a DES two-layer model as a semi-permeable membrane boundary that controls the transition rate from the coating (first layer) to the artery (second layer). Let us first discuss the problem of diffusion across a semi-permeable membrane within the general context of two-layer systems. We denote by P_{cross} the probability that, within a small time interval dt, a drug molecule arriving to the boundary from the first layer crosses it to the second layer. In the opposite direction (from the second layer back to the first), the crossing probability is unity. A semi-permeable membrane can be incorporated in Langevin dynamics simulations of layered systems in the following manner: Let us first consider the simpler case where the friction coefficient α is the same on both sides of the membrane, which is located at $x = x_m$. We follow the particle until it crosses the membrane ($x^n < x_m$ and $x^{n+1} > x_m$). In order to decide whether the particle should cross the boundary or be reflected from it, we draw a random number, R, from a uniform distribution between zero and one. We accept the new coordinate and velocity (x^{n+1}, v^{n+1}) if $R < P_{\text{cross}}$ (crossing), and reverse them to $(2x_m - x^{n+1}, -v^{n+1})$ if $R > P_{\text{cross}}$ (reflection). If α varies across the membrane, the algorithm is only slightly more complicated: The new coordinate and velocity

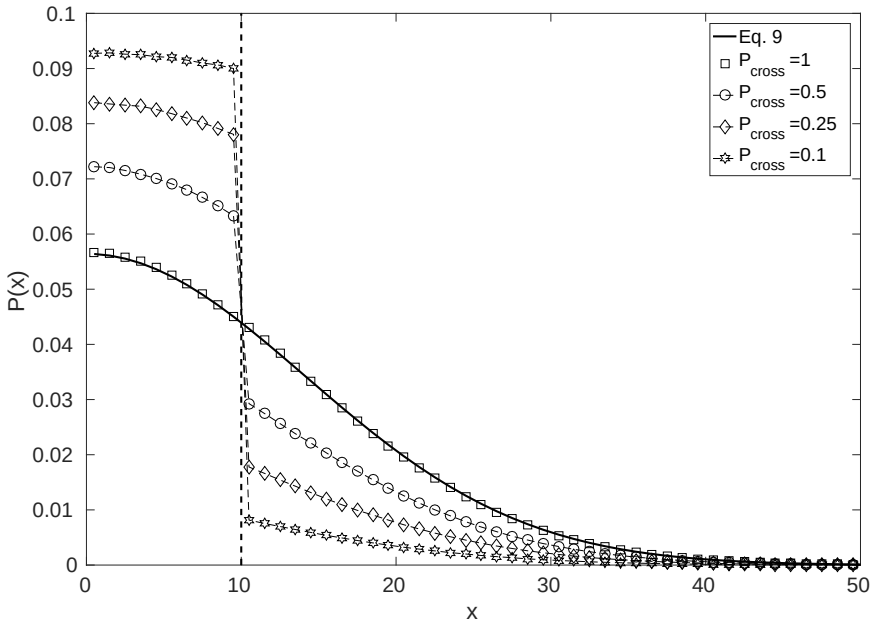

Figure 3.2: The PDF at $t = 100$ of a particle starting next to a reflecting wall at the origin, and diffusing through a semi-permeable membrane at $x = 10$ (represented by the vertical line), with crossing probability P_{cross}. Squares, circles, diamonds and stars denote the results of the Langevin dynamics simulations for $P_{\text{cross}} = 1, 0.5, 0.25, 0.1$, respectively. The solid line shows the solution for the case with no membrane [see Eq. (3.2)].

(x^{n+1}, v^{n+1}) are computed assuming that the friction varies in space, i.e., with the inertial convention for the average friction during the time step [Eq. (1.21)]. The step is accepted for $R < P_{\text{cross}}$ and is changed to a reflection step for $R > P_{\text{cross}}$. In the latter case, one must take into account the fact that the particle has not passed the membrane and, therefore, the friction coefficient along its trajectory remains constant. Therefore, the new coordinate and velocity are recalculated using the G-JF algorithm, with the already chosen value of β^{n+1}, but with the friction coefficient at the initial coordinate $x^n < x_m$. The recalculated (x^{n+1}, v^{n+1}) are accepted if the particle has not crossed the membrane ($x^{n+1} < x_m$), and changed to $(2x_m - x^{n+1}, -v^{n+1})$ if it has.

Fig. 3.2 shows simulation results for the PDF of a particle, initially located right next at a reflecting wall at $x = 0$, and diffusing in a medium with constant $D = 1$ that has a semi-permeable membrane at $x_m = 10$. The PDF at $t = 100$ is plotted for various values of P_{cross}.

The PDF is discontinuous at x_m because the membrane interferes with the diffusion rates. However, the membrane is not a probability sink or source and, therefore, the probability flux, $j(x) = -D\partial_x P(x,t)$, arriving at the membrane from left ($x \to x_m-$) is the same as the flux leaving the membrane to the right ($x \to x_m+$). This last feature of the PDF is visually apparent in Fig. 3.2. Since the membrane (partially) blocks the drug flow only from left to right, the probability density drops across the membrane, i.e., $P(x_m-,t) > P(x_m+,t)$. The data in Fig. 3.2 suggests that the following relation holds: $P_{\text{cross}} = P(x_m+,t)/P(x_m-,t)$. This relation is anticipated from the continuity of the flux and the fact that for each P_{cross} molecules crossing the membrane from left to right, one molecule passes from right to left. For $P_{\text{cross}} = 1$, the membrane is effectively non-existent because it does not impede the diffusion. In this limit, $P(x,t)$ becomes continuous at x_m and is given by Eq. (3.2) with $x_0 = 0$ (solid line in Fig 3.2).

3.4 Two-layer stent model

3.4.1 The model

Fig. 3.3 illustrates the simplest model for drug release from a DES. The model consists of two layers representing, respectively, the coating and the arterial wall. The first layer (coating), which has length L_1, is bounded between the stent strut ($x = -L_1$) and the stent topcoat ($x = 0$). The former is a reflecting boundary, while the latter is a thin semi-permeable membrane. The second layer (the arterial wall) is of length L_2. It is bounded between the topcoat and the adventitial side of the arterial wall ($x = L_2$), which is modeled as an absorbing boundary since the drug arriving at the end of the artery is lost in the tissues adjacent to the adventitia. The first and second layers have diffusion coefficients D_1 and D_2, respectively. We denote by m the mass of a drug molecule, and use the thermal energy k_BT as the energy scale of the problem.

Typical values for the system parameters are given in the second column of Table 3.1 in

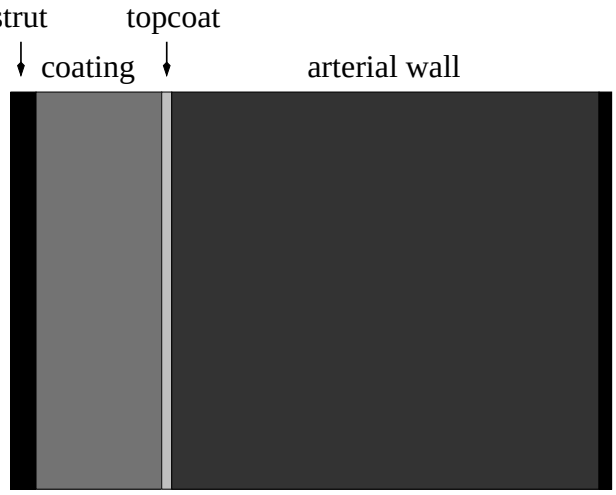

Figure 3.3: Schematics of the two-layer model for drug release from a DES.

parameter	physical value	normalized value	simulation value
L_1	$5 \times 10^{-6}\,\mathrm{m}$	1	1
L_2	$10^{-4}\,\mathrm{m}$	20	20
D_1	$10^{-17}\,\mathrm{m}^2/\mathrm{s}$	1/700	1/700
D_2	$7 \times 10^{-15}\,\mathrm{m}^2/\mathrm{s}$	1	1
k_BT	$4.3 \times 10^{-21}\,\mathrm{J}$	1	1
m	$1.5 \times 10^{-24}\,\mathrm{kg}$	6.8×10^{-19}	1
τ_1	$2.5 \times 10^{6}\,\mathrm{s}$	700	700
τ_2	$1.4 \times 10^{6}\,\mathrm{s}$	400	400
τ_m	$3.5 \times 10^{-18}\,\mathrm{s}$	9.7×10^{-22}	1/700

Table 3.1: Model parameters and their physical (second column), normalized (third column), and simulation (fourth column) values.

MKS units. In the third column, the same parameters are given in normalized units, where $L_1 = 1$, $D_2 = 1$, and $k_BT = 1$. Table 3.1 also gives the physical and normalized values of the time scales $\tau_i = L_i^2/D_i$ $(i = 1, 2)$, which are the characteristic diffusion times in each layer. Notice the interesting feature that these two time scales are of the same order of magnitude.

3.4.2 Using a fictitious mass

Another characteristic time scale appearing in table 3.1 is $\tau_m = mD/k_BT$, which is the crossover time from inertial to diffusive Langevin dynamics. This time scale, to be henceforth

referred to as the *ballistic time*, is very important from a computational perspective since Langevin dynamics simulations with the inertial interpretation must be run with time step $dt < \tau_m$ in order to appropriately simulate the transition statistics between the layers. In multi-layers systems, the limit on dt is set by the most viscous layer with the smallest diffusion coefficient and the smallest ballistic time. Therefore, in table 3.1, we only give τ_m of the first layer. For the stent model, we have $\tau_m \sim 10^{-18}$ sec, which is more than 24 orders of magnitude smaller than the diffusion times τ_1 and τ_2. This poses a huge computational challenge, as the aim of the study is to measure quantities like the rate of drug transfer to the bloodstream, which require simulations on time scales comparable to $\tau = \tau_1 + \tau_2$. This implies that each simulated trajectory requires, at least, 10^{24} time-steps, which would make the simulations prohibitively time consuming. More specifically, simulations of just 10^4 trajectories would require 10^{13} years (!) of CPU time on a state of the art PC.

The key to circumvent this outstanding computational problem is to notice that the diffusion equation (1.16) and Langevin's equation (1.12) yield the same long-time probability distributions if Einstein's relation $D(x)\alpha(x) = k_B T$ is satisfied. The mass of the particle, which only appears in Eq. (1.12), is unimportant for this relationship between the two equations to hold. Therefore, if we are only interested in obtaining the PDF at time scales comparable to τ, we can use a fictitious mass which is much larger than the actual mass and, thus, artificially increase the ballistic time τ_m. Of course, the artificial ballistic time must still be much smaller than the diffusion time, but τ_m does not need to be *negligibly* smaller than τ. In the fourth column of table 3.1 we give the normalized values of the model parameters used in our Langevin dynamics simulations of the DES model. The simulations values are identical to the normalized values for L_i, D_i, and $k_B T$, but the mass in the simulations is set to unity, i.e., about 18 orders of magnitude larger than the actual normalized mass of a drug molecule. This narrows the gap between the ballistic time and diffusion times to 5-6 orders of magnitude, and makes computationally feasible simulations of hundreds of thousands of trajectories with integration time-step $dt \ll \tau_m$.

3.4.3 Membrane permeability

In section 3.3 we defined P_{cross} to be the left-to-right crossing probability of the membrane in one time step. Since the time step of the simulations is typically several orders of magnitude smaller than the physical time scales of interest ($dt \ll \tau$), the crossing probability P_{cross} will generally be very small, which would considerably slow down the simulations. To circumvent this problem, as well as the problem arising from the difficulty to accurately estimate the crossing probability, we replace P_{cross} with a different measure for the membrane permeability - the permeation time T. The latter can be related to P_{cross} by noticing that each time the particle attempts to cross the membrane, it has probability P_{cross} to cross it and probability $1 - P_{\text{cross}}$ to be reflected. Thus, the probability of passing the membrane at the k-th attempt is $P_{\text{cross}}(1 - P_{\text{cross}})^{k-1}$, and the corresponding crossing time (measured from the time of the first crossing attempt) is $T_k = (k-1)\Delta$, where Δ is the return time between successive crossing attempts. This argument demonstrates that the permeation times are geometrically distributed, with an average crossing time $\langle T_k \rangle = \Delta(1 - P_{\text{cross}})/P_{\text{cross}}$. In reality, Δ is obviously not fixed but, itself, follows a certain continuous distribution. Therefore, the actual permeation time does not follow a discrete geometric distribution, but its continuous exponential analogue

$$p(t) = \frac{1}{T} \exp\left(-t/T\right), \tag{3.4}$$

where T is the characteristic permeation time. Similarly to its discrete counterpart $\langle T_k \rangle$, $T = \Delta(1 - P_{\text{cross}})/P_{\text{cross}}$, but here Δ denotes the *average* time between successive attempts. To account for the delay effect of a semi-membrane in simulations, we follow the trajectory of the particle assuming that the membrane is fully-permeable (i.e., as if there is no membrane present). At each crossing of the membrane we draw a random waiting time from the exponential distribution (3.4), and this delay time is simply added to cumulative time of the dynamics.

3.5 Results

The quantity of most interest for therapeutic applications is the rate of drug transfer from the stent coating to the arterial tissue. This can be characterized by the fractions $\Pi_1(t)$ and $\Pi_2(t)$ of drug present in the coating (layer 1) and the arterial wall (layer 2), respectively. These quantities are related to the PDF via

$$\Pi_1(t) = \int_{-L_1}^{0} P(x,t)dx, \tag{3.5}$$

$$\Pi_2(t) = \int_{0}^{L_2} P(x,t)dx. \tag{3.6}$$

In simulations, each trajectory is terminated upon arrival to the arterial wall boundary, which implies that $\Pi_1(t) + \Pi_2(t)$ is a monotonic function decreasing from unity at $t = 0$ to zero at $t \to \infty$. $\Pi_1(t)$ and $\Pi_2(t)$ are simply identified with the fraction of trajectories that at time t arrive at some point within the coating and arterial wall layers, respectively.

Fig. 3.4 shows our computational results for Π_1 (dashed curves) and $\Pi_2(t)$ (solid curves) as a function of the time t. The results are based on 2.1×10^5 trajectories simulated with time step $dt = 10^{-4}$ which meets the requirement $dt \ll \tau_m$ where $\tau_m = 1/700$ is the ballistic time (see table 3.1). The initial coordinates of these trajectories are chosen from a uniform distribution between $x = 0$ and $x = L_1$, which reflects the initial uniform distribution of the drug within the coating layer. The thin curves in Fig. 3.4 depict results for the DES model without a semi-permeable membrane, i.e., with vanishing permeation time $T = 0$ between the layers. Not surprisingly, Π_1 decreases monotonically from 1 to 0 on a time scale $t \sim 10^3$ ($\sim 10^3$ hours in physical units), which is comparable to the sum of diffusion times in the coating and the arterial wall $\tau = \tau_1 + \tau_2$. Π_2 increases from an initial value of 0, arrives to a maximum value for $t \lesssim 200$, and then monotonically decreases to 0 at larger times. The behavior of Π_2 reflects net drug transfer from the stent coating to the arterial wall at the beginning of the process, followed by gradual loss of drug at longer times, due to absorption in the tissues adjacent to the adventitia. The thick curves in Fig. 3.4 depict results for the

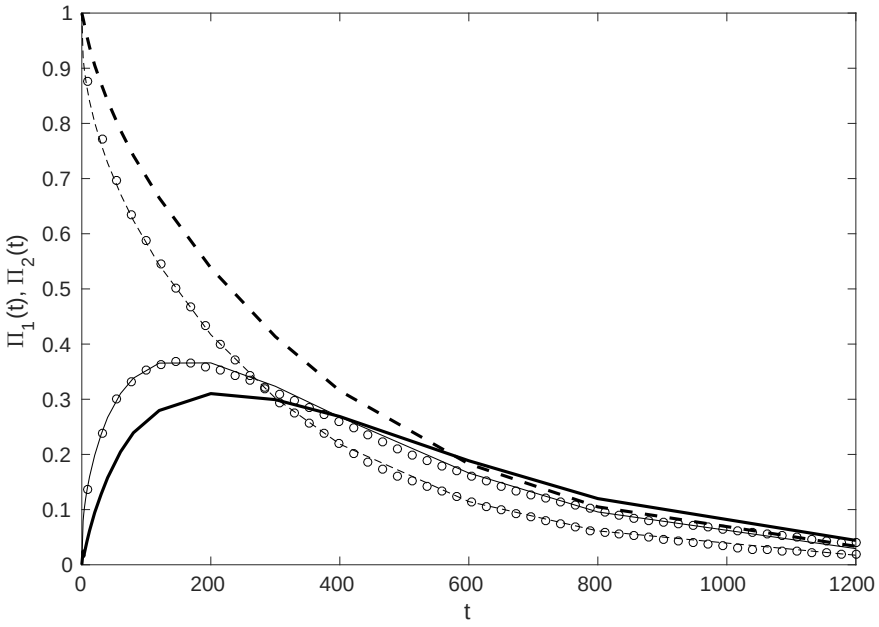

Figure 3.4: The fraction of drug in the coating (dashed curves), Π_1, and in the arterial wall (solid curves), Π_2, as a function of time. The thin and thick curves show simulation results for a DES with semi-permeable membranes having, respectively, characteristic permeation times $T = 0$ (no membrane) and $T = 10$. The circles represent the results of ref. [11] for the same DES model with identical model parameters (see footnote [97]).

same model but with a semi-permeable membrane characterized by permeation time $T = 10$. The results for Π_1 and Π_2 in this case exhibit trends similar to those observed in the $T = 0$ simulations.

The open circles in Fig. 3.4 depict the results derived in ref. [11] for the same DES model with identical model parameters (see footnote [97]). These results have been obtained by numerically solving the diffusion equation at each layer, subject to a similar initial condition at $t = 0$, and boundary conditions at $x = -L_1$ and $x = L_2$. At $x = 0$, the author of ref. [11] imposed (i) continuity of the flux and (ii) discontinuity in the concentration, with the concentration jump related, via the Kedem-Katchalsky equation [92], to the local flux and the membrane permeability. In this very different approach, the permeability also depends on the instantaneous drug concentrations on both sides of the membrane. Nevertheless, the results of ref. [11] exhibit a perfect agreement with our Langevin dynamics simulation results

for $T = 0$. The agreement can be attributed to the fact that the DES membrane has a nearly negligible effect on the rate of drug flow from the stent coating to the arterial wall.

3.6 Discussion

In this work we use underdamped Langevin dynamics simulations for solving the diffusion equation for a simple two-layer model of a drug-eluting stent (DES). To the best of our knowledge, this is the first attempt to derive the solution of a DES model using this approach. In fact, the application of underdamped Langevin dynamics simulations is also highly uncommon in other engineering and natural science areas dealing with the solution of complex diffusion equations. Much more common is the use of finite element and finite difference methods. These exist in a variety of forms, and the selection, design, and implementation of a method that best fits a given problem may be a complicated task. Langevin dynamics simulations constitute an alternative approach; however, the vast majority of studies of diffusion problems are based on simulations of the overdamped Langevin equation which neglect the inertial term on the r.h.s. of Eq. (1.12). This introduces complications stemming from the Itô-Stratonovich dilemma and the associated spurious drift. These complications can be addressed when $D(x)$ is a smooth function which varies only slightly during an integration time step, but not in simulations of layered systems where $D(x)$ is discontinuous. In the latter case, one must introduce decision rules for crossing the boundary between layers, even if those layers are *not* separated by a membrane. A Monte-Carlo algorithm implementing such types of decision rules has been recently presented [98], but we are not aware of a similar algorithm for overdamped Brownian dynamics. This extraordinary problem is completely avoided in underdamped Langevin dynamics simulations which, if run properly, produce correct thermal diffusion between sharp interfaces. Accurate solutions for a wide range of diffusion equations can be obtained by this approach with relative computational simplicity and accuracy, provided that one uses a robust integration scheme (such as the

G-JF integrator) together with a suitable convention rule for choosing the average α within a time-step of the simulations (e.g., the "inertial" convention). The merits of the approach are nicely exemplified in Fig. 3.4, which exhibits perfect agreement between the simulation results of this chapter and the predictions of ref. [11] for the same model.

The only parameter that needs to be tuned in the simulations is the mass of the diffusing particle whose value does not affect the PDF at the large time scales of interest associated with the diffusion problem. It must be selected such that the ballistic time $\tau_m = m/\alpha$ is much smaller, but not necessarily negligible, compared to the characteristic diffusion time. In one-dimensional multi-layer systems, the ballistic time is set by the friction coefficient of the most viscous layer, and the inertial convention for the average friction needs to be applied only when the particle moves between layers. However, the method can be readily implemented to diffusion problems in higher dimensions and can, without any special difficulty, be employed to study systems where the diffusion coefficient changes continuously in space. Such problems are generally more complicated for analytical treatment, as well as for other computational approaches.

The model studied in this chapter encompasses only two aspects of pharmacokinetics in the DES system, namely diffusion and crossing of a semi-permeable membrane. More recent studies suggest that advection, caused by a pressure gradient, and drug binding to receptor sites within the arterial wall may have a substantial effect on the rate of drug transport [78]. Both mechanisms can be dealt with within the underdamped Langevin dynamics simulation method presented in this work. Specifically, advection results from the action of a deterministic ("regular") force acting on the particle in addition to friction and thermal noise. In the presence of such a force, the full form of G-JF discrete-time equations (1.17 and 1.18) must be used. Drug binding can be dealt with by distributing binding sites and introducing a short-range attractive potential between the diffusing particle and the binding sites. The forces associated with the gradient of the binding potentials can then be accounted for via Eqs. (1.17) and (1.18). In a future publication we plan to investigate

model systems including these additional effects, in order to demonstrate the great potential of underdamped Langevin dynamics simulations for solving non-trivial diffusion problems.

We thank MD Carlos Cafri for helpful discussions about physiological aspects of the problem.

Chapter 4

Summary

In this thesis we utilize underdamped Langevin dynamics simulations for studying diffusion problems in systems with a spatially-varying friction coefficient. The results are obtained using the statistically accurate and robust G-JF algorithm [32,33]. In heterogeneous systems, one needs to choose an interpretation for the effective friction at each time step, since the value of $\alpha(x)$ changes when the particle moves. The ambiguity about the appropriate choice of the friction is known as the "Itô-Stratonovich dilemma". Despite the name (which follows from the most commonly used interpretations of Itô [26] and Stratonovich [27]), when using the overdamped equation (1.13), it is the Hänggi (or "isothermal") convention [29] that produces the correct isothermal Fickian dynamics [23]. The advantage of keeping the inertial term in Eq (1.12) is that it ensures that all reasonable interpretations of the stochastic calculus lead to the same, correct, PDF when $dt \to 0$. This is due to the fact that, unlike the overdamped equation, the underdamped equation depicts continuous motion that correctly captures the inertial part of the dynamics at short time scales as well. This is essential for producing the drift that the particle experiences toward the low friction end of the system. In the overdamped limit, a spurious drift term (that depends on the chosen convention) must be added to the equation. Our simulation results are based on the G-JF algorithm [32, 33] with the newly proposed "inertial" convention [22, 24] that generates accurate results even

for relatively large time steps.

The benefits of using the underdamped Langevin equation (1.12) become apparent when dealing with cases where $\alpha(x) \to 0$. This case, discussed in chapter 2, is an example of precisely the scenario in which the overdamped equation (1.13) is most inaccurate, i.e., when the ballistic term is not negligible compared to the friction term even at long times. In such cases, the overdamped description can lead to erroneous results that violate basic physical principles, e.g., motion with an ever-increasing velocity (hyper-diffusion). The underdamped equation (1.12) produces correct dynamics.

Another scenario where the underdamped framework is advantageous is where the friction varies rapidly. The extreme example of this is diffusion in layered systems, where the friction function is discontinuous. In the overdamped framework, the particle does not move continuously, but rather "hops" from one location to another. Therefore, boundary decisions must be taken when, in overdamped simulations, the particle crosses a friction interface. In underdamped Langevin dynamics simulations, such boundary decisions are unnecessary, since in these simulations (with a not too large dt) the particle moves continuously between different layers.

We conclude by noting that most of our knowledge about heterogeneous diffusion is limited to one-dimensional systems. In the future, it will be interesting to investigate model systems in higher dimensions, in particular anisotropic systems where the principle directions of the friction *tensor* vary in space. We hope to show that the G-JF algorithm can be naturally expanded for Langevin dynamics in such systems. Another interesting extension is the dynamics of rod-like molecules, in which the intra-molecular distances are constrained.

Appendix A

Diffusion in higher dimensions

In dimensions higher than one, Eq. (1.16) is generalized to:

$$\frac{\partial P(\vec{r},t)}{\partial t} = \sum_{i=1}^{d}\sum_{j=1}^{d} \frac{\partial}{\partial r_i} D_{ij}(\vec{r}) \frac{\partial P(\vec{r},t)}{\partial r_j}, \tag{A.1}$$

where $\vec{r}$ denotes the position vector and r_i denote orthogonal coordinates. Here $D_{ij}(\vec{r})$ is the (symmetric) diffusion tensor, whose components may be coordinate-dependent. If one considers a d-dimensional system with radial symmetry and assumes that the particle begins at the origin of symmetry, $P(\vec{r},0) = \delta(\vec{r})$, then $P(\vec{r},t) = P(r,t)$, where $r = |\vec{r}|$, and Eq. (A.1) simplifies to

$$\frac{\partial P(r,t)}{\partial t} = \frac{1}{r^{d-1}} \frac{\partial}{\partial r} \left(D(r) r^{d-1} \frac{\partial P(r,t)}{\partial r} \right). \tag{A.2}$$

Notice that $P(r,t)$ is the probability density per d-dimensional unit volume. For $D(r) = D_0 \left| r/l \right|^c$, the solution of Eq. (A.2) with the delta function initial condition is [64]

$$P(r,t) = \frac{\Gamma\left(\frac{d}{2}\right) \left[(2-c)^{2(d-1)+c} \left(D_0 t\right)^d \right]^{1/(c-2)}}{2\pi^{\frac{d}{2}} \Gamma\left(\frac{d}{2-c}\right)} \exp\left[\frac{-r^{2-c}}{(2-c)^2 (D_0 t)} \right], \tag{A.3}$$

and for brevity we set $l = 1$. In this case, The MSD is given by

$$\left\langle \Delta r^2 \right\rangle = \int_0^\infty r^2 P(r,t) \frac{2\pi^{\frac{d}{2}}}{\Gamma\left(\frac{d}{2}\right)} r^{d-1} dr = d \frac{\Gamma\left(\frac{3}{2-c}\right)}{\Gamma\left(\frac{1}{2-c}\right)} \left[(2-c)^2 D_0 t\right]^{2/(2-c)}. \tag{A.4}$$

Not surprisingly, this result shows that $\langle \Delta r^2 \rangle = d \langle \Delta x^2 \rangle$, where $\langle \Delta x^2 \rangle$ is the MSD along one of the Cartesian coordinates (see Eq. (2.9)).

Bibliography

[1] R. Brown, Philos. Mag. **4**, 161 (1828)

[2] A. Einstein, Ann. Phys. (Leipzig) **17**, 549 (1905).

[3] N. G. van Kampen, *Stochastic Processes in Physics and Chemistry* (North-Hollans, Amsterdam, 1981).

[4] W. T. Coffey, Y. P. Kalmyfov, and J. T. Waldron, *The Langevin Equation: with application in Physics, Chemistry, and Electrical Engineering* (World Scientific, London, 1996).

[5] R. W. Ballufi, S. Allen, W. C. Carter, *Kinetics of Materials* (Wiley, Hoboken NJ, 2005).

[6] B. Gebhart, *Heat Conduction and Mass Diffusion* (McGraw-Hill, New York NY, 1993).

[7] F. Perrin, Journal de Physique. **7**, 1 (1936).

[8] K. Berg-Sorenson, Y. Castin, E. Bonderup and K. Molmer, J. Phys. B-At Mol. Opt. **25**, 4195 (1992).

[9] P. C. Fiss and E. J. Zajac, Admin. Sci. (Leipzig) **49**, 501 (2004).

[10] Ricciardi and M. Luigi, *Diffusion Processes and Related Topics in Biology* (Springer-Verlag, Berlin, 1977).

[11] G. Pontrelli and F. de Monte, Heat Mass Transfer. **50**, 3658 (2007).

[12] J. Corish and O.I. Corrigan, J. Chem. Soc. **86**, 1317 (1990).

[13] P. Sharma, S. Ghosh, S. Bhattacharya, Appl. Phys. Lett., **97**, 104101 (2010).

[14] P. Langevin, C. R. Acad. Sci. (Paris) **146**, 530 (1908).

[15] J. Philbert, Diffusion Fundmantals. **2**, 1 (2005)

[16] G. Parisi, *Statistical Field Theory* (Addison Wesley, Menlo Park, 1988).

[17] R. Kubo, Rep. Prog. Phys. **29**, 255 (1966).

[18] W. M. Haynes, *CRC Handbook of Chemistry and Physics* (CRC Press, Boca Raton FL, 2012).

[19] P. Lançon, G. Batrouni, L. Lobry, and N. Ostrowsky, Europhys. Lett. **54**, 28 (2001).

[20] G. Volpe, L. Helden, T. Brettschneider, J. Wehr, and C. Bechinger, Phys. Rev. Lett. **104** , 170602 (2010).

[21] R. Mannella and V. P. E. McClintock, Fluct. Noise Lett. **11**, 1240010 (2012).

[22] O. Farago and N. Grønbech-Jensen, Phys. Rev. E **89**, 013301 (2014).

[23] A. W. C. Lau and T. C. Lubensky, Phys. Rev. E **76**, 011123 (2007).

[24] O. Farago and N. Grønbech-Jensen, J. Stat. Phys. **156**, 1093 (2014).

[25] J. L. Domb, Ann. Math. **43**, 351 (1942).

[26] K. Itô, Proc. Imp. Acad. **20**, 519 (1944).

[27] R. L. Stratonovich, Siam J. Control. **4**, 362 (1966).

[28] H. Risken, The Focker-Planck Equation (Springer-Verlag, Berlin, 1988).

[29] P. Hänggi, Helv. Phys. Acta **51** , 183 (1978).

[30] Stochastic differential equations can be used to describe different processes in diverse fields, such as biology, economy, neuroscience, geophysics, and more. For many applications, other interpretations (e.g., Itô or Stratonovich) may be appropriate. Here, we consider the physical problem of a particle's dynamics in isothermal systems, for which the relevant interpretation is the one of Hänggi. When the particle moves in a potential energy field $U(x)$, a force term $f(x) = -dU/dx$ should be added to the r.h.s. of Eq. (1.12). At large times, one expects to approach the equilibrium Boltzmann distribution function $P(x) \sim \exp\left[-U\left(x\right)/k_B T\right]$, which does not depend on the diffusivity function $D(x)$. This is achieved with the Hänggi convention, while other interpretations require the addition of a spurious drift term to the Langevin equation (see [22, 23] for a more detailed discussion).

[31] Most generally, it is possible to take a weighted average of the friction at the beginning and end of the time step. Denoting by $0 \leq \gamma \leq 1$ the weight of the end point friction, the general 'diffusion' equation is $\partial P(x,t)/\partial t = \partial/\partial x \left(D(x)^{\gamma} \partial/\partial x \left(D(x)^{1-\gamma} P(x,t)\right)\right)$. One can easily verify that the Itô convention corresponds to $\gamma = 0$ (Eq. 1.14), the Stratonovich convention corresponds to $\gamma = 0.5$ (Eq. 1.15) and the Hänggi convention corresponds to $\gamma = 1$ (Eq. 1.16). See [23] for a more detailed discussion.

[32] N. Grønbech-Jensen, and O. Farago. Mol. Phys. **111**, 983 (2013).

[33] N. Grønbech-Jensen, N.R. Hayre, and O. Farago, Comput. Phys. Commun. **185**, 524 (2014).

[34] S. Regev, N. Grønbech-Jensen and O. Farago, Phys. Rev. E **94**, 012116 (2016).

[35] E. Koscienly-Bunde, A. Bunde, and S. Havlin, Phys. Rev. Lett. **81**, 729-732 (1998).

[36] R. Berkowicz, Boundry-Layer Meteorol. **30**, 201-219 (1984).

[37] V. Plerou, P. Gopikrishnan, L.A.N. Amaral, et. al, Phys. Rev. E **62**, 0210513 (2000).

[38] S. Havlin and D. Ben-Avraham, Adv. Phys. **51**, 187-292 (2002).

[39] J. Jeon, N. Leijnse, L.B. Oddershede, and R. Metzler, New J. Phys. **15**, 045011 (2013).

[40] Y. Sagi, M. Brook, I. Almog, and N. Davidson, Phys. Rev. Lett. **108**, 093002 (2012).

[41] P.G. de-Gennes, *Scaling Concepts in Polymer Physics* (Cornell, Ithaca NY, 1988).

[42] M. Doi and S.F. Edwards, *The Theory of Polymer Dynamics* (Oxford Uni., New York NY, 1989).

[43] B.M. Regner, D. Vucinic, C. Domnisoru, et. al, Biophys. J. **104**, 1652-1660 (2013).

[44] I. Bronstein, Y. Israel, E. Kepten, et. al, Phys. Rev. Lett. **104**, 018102 (2009).

[45] A. Sharifi-Viand, J. Elechtroanal. Chem. **671**, 51-57 (2012).

[46] X. Wu and A. Libacher, Phys. Rev. Lett. **84**, 3017-3020 (2000).

[47] A.M. Reynolds, Physica A **390**, 245-249 (2011).

[48] H. Scher and E.W. Montroll, Phys. Rev. B **12**, 2455 (1975).

[49] J. Masoliver, M. Montero, and G.H. Weiss, Phys. Rev. E **67**, 021112 (2003).

[50] R. Metlzer, J. H. Jeon, A. G. Cherstvy, and E. Barkai, Chem. Phys. **16**, 24128 (2014).

[51] K. B. Oldham, J. Spanier. *The fractional calculus* (Academic Press, New York NY, 1974).

[52] I. Podlubny. *Fractional Differential Equations* (Academic Press, New York NY, 1998).

[53] R. Metzler, J. Klafter, and I.M. Sokolov, Phys. Rev. E **58**, 581621 (1998).

[54] M. F. Shlesinger, Joseph Klafter. Chapter Levy Walks Versus Levy Flights in *On Growth and Form*. H. E. Stanley and N Ostrowsky. (Springer-Verlag, Berlin, 1986).

[55] M. Chi, E. Neal, G.K. Young, Water Resour. Res. **9**, 1523-1533 (1973).

[56] J. Beran, *Statistics for Long-Memory Processes* (Chapman & Hall, London, 1994).

[57] R. Metzler, E. Barkai, and J. Klafter, Phys. Rev. Lett. **82**, 3565-3567 (1999).

[58] R. Metzler and J. Klafter Phys. Rep. **339**, 1-77 (2000).

[59] G. Sikora, K. Burnecki, and A. Wylomańska, Phys. Rev. E **95**, 032110 (2017).

[60] A. Elhanbaly, Chaos, Solitons, Fractals **54**, 455 (2002).

[61] K.S. Fa and E.K. Lenzi, Phys. Rev. E **67**, 061105 (2003).

[62] A. G. Cherstvy , A. V. Chechkin, and R. Metzler , New J. Phys. **15**, 083039 (2013).

[63] T. Sandev, A. Schulz, H. Kantz, and A. Iomin, cond-mat, 1704.07000 (2017).

[64] B. O'Shaughnessy and I. Procaccia, Phys. Rev. Lett. **54**, 455 (1985).

[65] R.D. Safian and S.C. Textor, N. Engl. J. Med. **344**, (2001), 431-442.

[66] C.T. Dotter, R.W. Buschman, M.K. McKinney, Radiology **147**, (1983), 259-260.

[67] M.A. Costa, A. Abizaid, A.G.M.R. Sousa and J.E. Sousa, Chapter 22 in *Essentials of Restenosis For the Interventional Cardiologist*. Eds. H.J. Duckers, E.G. Nabel and P.W. Serruys (Human Press, Totowa NJ, 2007).

[68] M. Joner, A.V. Finn, A. Farb, et al., J. Am. Coll. Cardiol. **48**, (2006), 193-202.

[69] A. Roguin., Circulation: Cardiovascular Interventions. **4**, (2011), pp. 206-209.

[70] C. Vergara and P. Zunino, M.M.S. **7**, (2008), 565-588.

[71] G. Pontrelli and F. de Monte, Heat Mass Transfer. **53**, (2010), 3629-3637.

[72] S. McGinty, Math. Biosci. **257**, (2014), 80-90.

[73] G. Pontrelli and F. de Monte, Math. Biosci. **257**, (2014), 96-103.

[74] S. McGinty, T.T.N. Vo, M. Meere, et al., Acta Biomaterialia **18**, (2015), 213-225.

[75] S. McGinty and G. Pontrelli, J. Control. Release. **217**, (2015), 327-336.

[76] S. McGinty, M. Wheel, M. Meere, S. McKee, and C. McCormick, Int. J. Heat Mass Transf. **90** (2015) 266-279.

[77] J.A. Ferriera, J. Naghipoor and P. de Oliviera, Math. Med. Biol. **33**, (2016), 329-357.

[78] S. McGinty and G. Pontrelli G., J Math Chem. **54**, 2016, 967-976.

[79] G. Pontrelli and F. de Monte, J. Porous Media **12**, (2009), 19-28.

[80] S. McGinty, S. McKee, R.M. Wadsworth, and C. McCormick, Math. Med. Biol. **28**, (2011), 1-29.

[81] C. D'Angelo and P. Zunino, Esaim-Math. Model. Num. **54**, (2011), 447-476.

[82] S.S. Hossain, S.F.A. Hossainy, Y. Bazilevs, et al., Comput. Mech. **45**, (2012), 213-242.

[83] G. Pontrelli, A. Di Mascio, and F. de Monte, Heat Mass Transfer. **66**, (2013), 844-854.

[84] A.P. Mandal, Sarifuddin, and P.K. Mandal, Appl. Math. Comput. **266**, (2015), 968-981.

[85] A. Seidlitz, S. Nagel, B. Semmling, et al., Eur. J. Pharm. Biopharm. **78**, (2011), 36-48.

[86] McGinty S, S. McKee, R.M. Wadsworth and C. McCormick, Siam J. Appl. Math. **73**, (2013), 2004-2008.

[87] R.I. Hickson, S.I. Barry, and G.N. Mercer, Heat Mass Transfer. **52**, (2009), 5776-5783.

[88] R.I. Hickson, S.I. Barry, and G.N. Mercer, Heat Mass Transfer. **52**, (2009), 5784-5791.

[89] M. d'Errico, P. Sammarco and G. Vairo, Math. Biosci. **267**, (2015), 79-96.

[90] M.R. Rodrigo, and A.L. Worthy, J. Math. Anal. Appl. **444**, (2016), 475-502.

[91] M. Grassi, G. Pontrelli, L. Teresi, et al., Math. Biosci. **6**, (2009), 493-508.

[92] P. Zunino, Cardiov. Eng.: Int. J. **4**, (2004), 181-191.

[93] A. Garon and M.C. Delfour, Siam J. Appl. Math. **74**, (2014), 1354-1374.

[94] C. Creel, M. Lovich, and E. Edelman, Circ. Res. **86**, (2000), 879-884.

[95] C. Hwang, D. Wu, and E.R. Edelman, Circulation **104**, (2001), 600-605.

[96] B.M. O'Connel and M.T. Walsh, Ann. Biomed. Eng. **38**, (2010), 1354-1366.

[97] The only model parameters not having identical values to those in [11] are the layers diffusion coefficients D_1 and D_2 whose values here are 10^3 times smaller than in [11]. The values quoted in [11] correspond to characteristic diffusion times τ_1 and τ_2 that are unrealistically low (hours rather than weeks). The values of D_1 and D_2 used here agree with more recent estimates, see e.g. [72]. This change does not affect the comparison of our solution for $\Pi_1(t)$ and $\Pi_2(t)$ with the data visually extracted from Fig. 3 in ref. [11], because the results throughout this chapter are plotted in normalized units. Notice that the definition of the normalized time unit is different here ($\tau_2 = 400$) than in ref. [11] ($\tau_2 = 1$). The data from [11] is plotted in Fig. 3.4 after conversion to the time units used in this work (i.e., multiplication by a factor of 400).

[98] H.W. de Haan and M.V. Chubynsky, arXiv:1208.5081 (2012).